EXPERIMENTAL AND NUMERICAL STUDY OF THE SWIRLING FLOW IN CONICAL DIFFUSERS

Rodrigo Queiroz Neiva, neivarq@gmail.com
Aldo João de Sousa, aldo@unb.br
José Gustavo Coelho, josegustavo@unb.br
Antonio C. P. Brasil Junior, brasiljr@unb.br
Universidade de Brasilia
Departamento de Engenharia Mecânica
Laboratório de Energia e Ambiente
Campus Darcy Ribeiro, Brasilia – DF, Brasil

Abstract. *The aim of the present work is to analyze experimental and numerically the swirling turbulent flow in conical diffusers. This theme is impotant in several fields of the engineering, especially in the hydraulic turbines, cyclones, combustors and atmospheric flows. The work is developed in two different fronts. In the first, Particle Image Veocimetry- PIV is used in order to obtain information of the mean flow, in the axial and also in the cross sections of the swirling flow. In each PIV plane, two velocity components are obtained. In the second stage a numerical study, using the same conditions for the experimental water flow is done. These results obtained in those two parts will be accomplished also to show the efficiencey of the numerical method.*

Keywords*: PIV, RANS, Swirling Flow, Turbulence.*

1. INTRODUCTION

The diffusers are used to reduce the flow speed and to increase its static pressure, in other words, to convert kinetic energy in pressure energy. With this important characteristic the diffusers present several applications in different engineering branches, including hydroelectric turbines, exhausters, cyclones, combustors, among many other applications.

Another subject that shows great interest, in the current days, is the analysis of swirling flows, generated by turbine rotors, guidelines blades in the hydraulic machines and combustors, and cyclones. There is in the literature countless works on those important themes, as the work accomplished by Hach (1983), where calculations are made for different diffusers and the influence of the insertion of the swirl at the entrance of the diffuser is also evaluated; Azad et al (1989) present an analysis of diffuser flow, with emphasis in the aspects of turbulent flow; Ishizaka (1993) presents a study using CFD (Computational Fluid Dynamics) in diffusers of gas turbines; Clausen et al (1993) evaluate the development of the swirl flow in the turbulent boundary layer of a conical diffuser; Edwards et al (1993) compare two experimental techniques to quantify the swirl in the entrance of an annular diffuser.

Some more current works also deserve prominence, as accomplished by Japikse (2000) that determines the correlation between the swirls geometry and the aerodynamic for the efficiency of an annular diffuser. And Iaccarino (2000), that compares the results obtained by different commercial solvers in the study of the turbulence in diffuser flows; Coelho et al. (2006a), that make an expressive analysis of the influence of the swirl in the development of diffuser flow; Coelho et al. (2006b) that accomplishes a transient study of the conical diffuser flows.

In most of the cases where diffusers are used, it is important to evaluate the amount of pressure that the diffuser is able to recover. That is directly related with the stall of the boundary layer and recirculation produced in the central region of the diffuser. Those factors are directly related to the income of the diffuser. It is considered the separation of the boundary layer being function of the conditions at the entrance of the diffuser, the exit conditions, the Reynolds number, the Mach number, and also on the geometry of the diffuser. According to Blevins (1984), when the number of Reynolds is above 5×10^4, the flow separation becomes a function basically of the diffuser geometry. However, when a swirl is placed in the flow the situation will vary. If the rotation is small there will be a displacement of the boundary layer. If the rotation is large, recirculation will be present in the central flow zone.

This work presents experimental and simulated flow results for two different diffuser geometries, including longitudinal and secondary flow results, in different cross sections of the test section. The two studied diffusers present total angles of 10^o and 20^o, and the area ratio isn't altered.

For the numerical simulation it is used the SOLIDWORKS® package, for the generation of the geometry, and CFX-10 of ANSYS, for the mesh generation, as well to impose the flow boundary conditions, processing and post-processing. The RANS modeling is adopted (Reynolds Averaged Navier-Stokes) to model the turbulence. Another factor that influences the choice of this turbulence model is the good results presented by this methodology, even without the use of computers of great capacity. The chosen turbulence model was SST (Shear Stress Transport),

because this model brings in its formulation a combination of the best qualities of the other two closing models of first order.

2. GOVERNING EQUATIONS, TURBULENCE MODEL AND NUMERICAL METHODOLOGY

The governing equations of the analyzed flow are the averaged continuity equation and the momentum equation shown below:

$$\frac{\partial}{\partial x_j}\left(\overline{u_j}\right) = 0; \tag{1}$$

$$\frac{\partial}{\partial t}\rho\left(\overline{u_j}\right) + \frac{\partial}{\partial x_k}\rho\left(\overline{u_j}\,\overline{u_k}\right) = -\frac{\partial \overline{p}}{\partial x_i} + \frac{\partial \overline{\tau_{ij}}}{\partial x_i} + \frac{\partial}{\partial x_k}\rho\left[\nu_\tau\left(\frac{\partial \overline{u_j}}{\partial u_k} + \overline{\frac{\partial u_k}{\partial u_j}}\right)\right], \tag{2}$$

where u_i are the velocity components, ρ the density, p is the pressure, τ_{ij} is the viscous stress tensor, and ν_τ is the turbulent viscosity, that will be modeled inside of a closure context in first order, using the model SST.

The SST model was created originally by Menter et al (1994). It possesses two groups of transport equations that alter, depending on the analyzed region. If the analysis is close to the wall, it uses the *κ-ε* formulation, if it does not use *k-w* formulation. In the following it is shown the additional transport equations of this model:

$$\rho\frac{\partial k}{\partial t} + \rho\overline{u_j}\frac{\partial k}{\partial x_j} = \frac{\partial}{\partial x_j}\left[\left(\mu + \frac{\mu_t}{\sigma_k}\right)\frac{\partial k}{\partial x_j}\right] + \widetilde{P}_k - \beta^* \rho\kappa\omega, \tag{3}$$

where:

$$P_k = \mu_t \frac{\partial u_i}{\partial x_j}\left(\frac{\partial u_i}{\partial x_j} + \frac{\partial u_j}{\partial x_i}\right) \Rightarrow P_k = \min(P_k, 10\cdot\beta^*\rho\kappa\omega); \tag{4}$$

$$\rho\frac{\partial \omega}{\partial t} + \rho\overline{u_j}\frac{\partial \omega}{\partial x_j} = \frac{\partial}{\partial x_j}\left[\left(\mu + \sigma_\omega\mu_t\right)\frac{\partial \omega}{\partial x_j}\right] + \alpha\rho S^2 - \beta\rho\omega^2 + 2(1-F_1)\rho\sigma_{w2}\frac{1}{\omega}\frac{\partial \kappa}{\partial x_i}\frac{\partial \omega}{\partial x_i}, \tag{5}$$

where F_1, aims the determination of the constants in the model and also the variation of the transport equation of ω . Consequently, F_1 is defined as:

$$F_1 = \tanh\left\{\left\{\min\left[\max\left(\frac{\sqrt{\kappa}}{B^*\omega y}, \frac{500\nu}{y^2\omega}\right), \frac{4\rho\sigma_{\omega 2}\kappa}{CD_{\kappa\omega}y^2}\right]\right\}^4\right\}, \tag{6}$$

with

$$CD_{\kappa\omega} = \max\left(2\rho\sigma_{\omega 2}\frac{1}{\omega}\frac{\partial \kappa}{\partial x_i}\frac{\partial \omega}{\partial x_i}, 10^{-10}\right), \tag{7}$$

and y is the distance of the sliding surface.

The other constants are all originated from the κ – ε e κ – ω models, with some fittings, being determined as: β*= 0,09, α_1 =5/9, β_1 = 3/40, σ_{k1}= 0,85, $\sigma_{\omega 1}$ = 0,5, α_2 =0,44, β_2 = 0,0828, σ_{k2} = 1 e $\sigma_{\omega 2}$ = 0,856. (Menter, 2003).

The turbulent viscosity is calculated by means of the following equation:

$$\mu_t = \rho\frac{a_1 k}{\max\left(a_1\omega, \left(S_{ij}S_{ij}\right)^{\frac{1}{2}}F_2\right)}; \tag{8}$$

where $\left(S_{ij}S_{ij}\right)^{\frac{1}{2}}$ is an invariant measure of the rate of the strain tensor and F_2 is one of the combination equation determined by Eq. 9 having the aim to model the change in the turbulent viscosity formulation, depending on the flow region in analysis .

$$F_2 = \tanh\left\{\left[\max\left(\frac{2\sqrt{\kappa}}{B^* \omega y}, \frac{500\nu}{y^2\omega}\right)^2\right]\right\}. \tag{9}$$

The software used in the present work, the CFX 10, uses the method of the finite volumes. The test section that comprises the computational domain is shown in Fig. 1. In this figure it is shown the inlet, upstream of the swirl, the own swirl, and its position in the flow, the diffuser with its total angle, and the exit section, downstream of the diffuser.

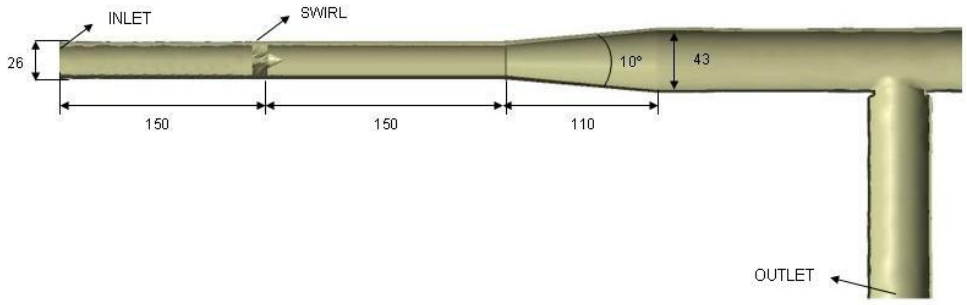

Figure 1: Test section of a diffuser of total angle of 10º (distances in mm).

A similar diffuser, with a total angle of 20º, was also tested and simulated. Starting from the two built geometries used in the experimental test section a 3-D solid is obtained, from the SOLIDWORKS®. With these diffuser geometries, the software CFX-10 is employed to generate the meshes for the simulations. The boundary conditions utilized in the simulation consist in impose the same flow rate in the entrance and in the exit of the test section used in the experimental measurements and also the no slip condition on the walls.

3. EXPERIMENTAL APPARATUS

In this work two diffuser geometries, one with total angle of 10^o and the other with total angle of 20^o are tested and simulated. Water flows in the diffuser in a closed circuit. The water flow rate in the test section is controlled by a frequency inverter, coupled to the motor of the centrifugal pump. The flow rate is measured by a rotameter. A water reservoir of 0,3 m^3, open to the atmosphere, feeds the test section and also receives the returning water. Seeding particles of appropriate size and density for PIV - Particle Image Velocimetry are inserted in the water tank, in appropriate concentration and circulate with the water. Longitudinal measurements in the diffusers as well as transversal measurements in the test sections are accomplished. In each two-dimensional PIV measurements two orthogonal velocity components are obtained. For the measurement in a longitudinal plan of the diffuser a laser light sheet illuminates the test section horizontally, and the digital camera is placed with its axis in the vertical direction. For the measurement of components of speed in a transversal flow, the light sheet illuminates a vertical cross section and the digital camera now has its axis in the same direction of the diffuser axis. The light sheet is obtained with the aid of a cylindrical lens, coupled at the exit of the laser cavities. In the PIV system, utilized in this work, two pulsed laser cavities type Nyodim-YAG, with wavelength of 532 nm (green color) and maximum frequency per cavity equal to 15 Hz operates in a synchronized way with the digital camera. This synchronization is made with a time hub. Appropriate software is responsible for the command, control, image acquisition and processing of the whole PIV process. This equipment is produced by IDT – Systems. In the present work, the acquisition frequency is set in 6 Hz and a group of 200 image-pairs were used for obtaining two mean velocities of the flows. Instantaneous flow characteristics are also obtained. In the PIV process, each image covering an area of 60 mm x 60 mm is subdivided in a group of 75 x 75 interrogation areas and, for each interrogation area, a velocity vector is associated.

4. RESULTS AND DISCUSSION

Figure 2 presents the three-dimensional simulated flow result in a split way, between the swirler and the diffuser, and also inside the own diffuser, to facilitate the visualization. This simulation shows a typical turbulent flow that, when

passing trough the swirler starts to present a swirling flow, rotating in a clockwise movement. The legend shows the intensity of the velocity vector.

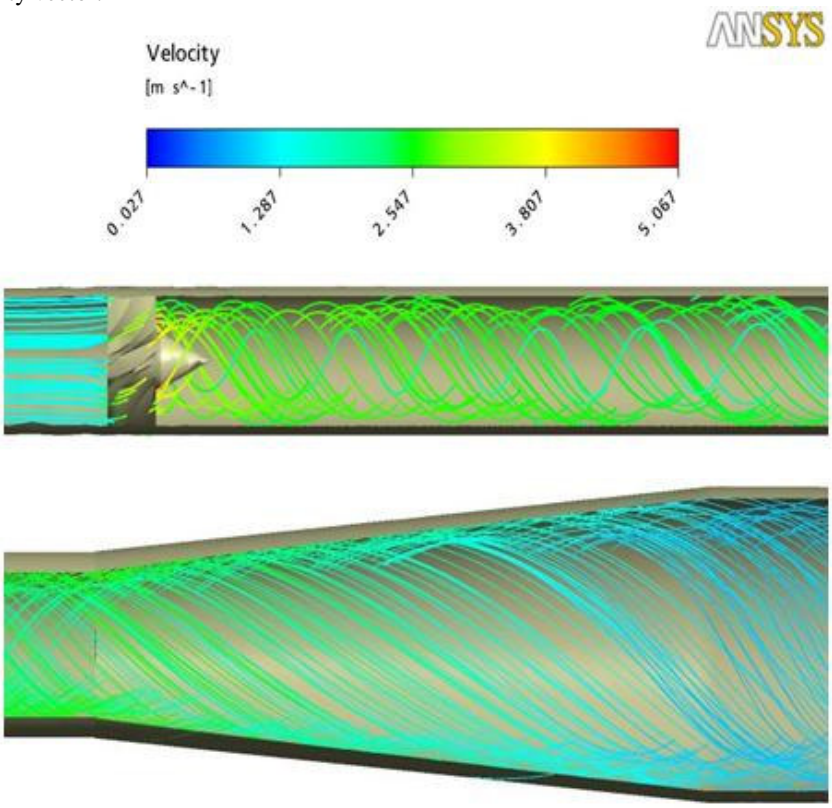

Figure 2: Tridimensional swirling flow between the swirl and the 10^{o} diffuser, and also inside the diffuser.

Figure 3 and Figure 4 present experimental PIV results in the two cross sections between the swirler and the diffuser and also in the own diffuser with total angle of 20º . In the experiment the water flow rate was set in 40 liters per minute and the swirler was installed at 200 mm of the diffuser entrance. It was chosen, in this case, cross sections at four different lontitudinal positions, to show the results obtained from the experimental measurements, which are, at 80mm of the swirler, 140 mm of the swirler, 30 mm from the diffuser entrance, and also at 50 mm of the diffuser entrance. Only the intensity of the horizontal velocity component is shown in each figure, all of them being expressed in m/s. Those flows are related to the secondary flows that occur in each cross section, and serves to show how the water is rotating in each of this visualized cross section. The vertical velocity components in those flow present very close measured values compared to the horizontal components, and identical results in the numerical simulations.

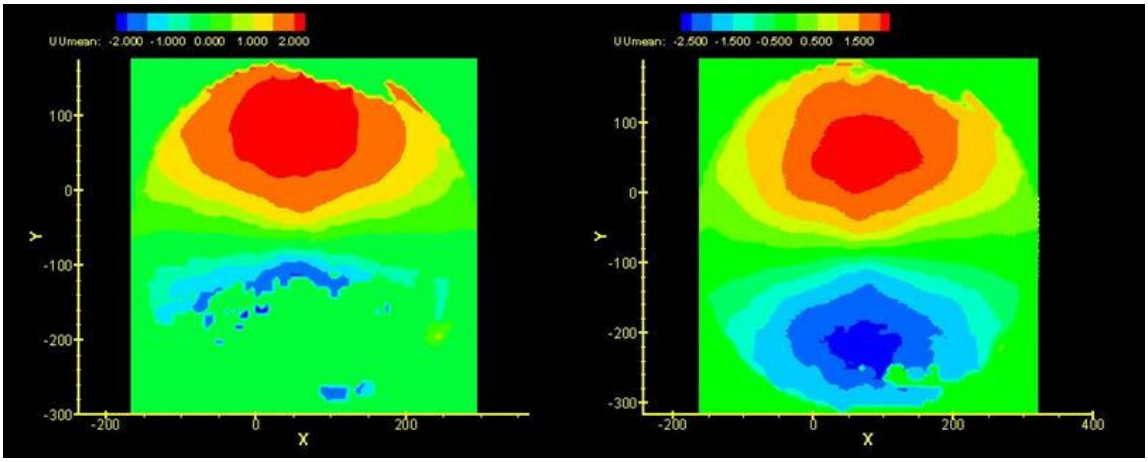

Figure 3: Horizontal velocity components for the de 20º diffuser, on the cross sections at 80 mm and 140 mm from the swirler exit.

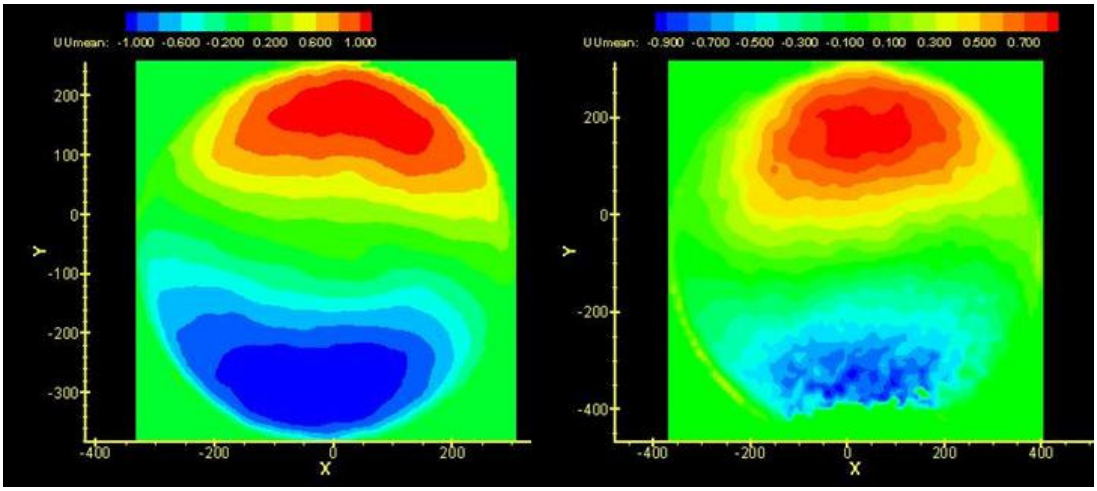

Figure 4: Horizontal velocity components inside the 20º diffuser, on the cross sections at 80 mm and 140 mm from its entrance.

The experimental results show a secondary flow rotating clockwise, with higher intensity in the regions close to the diffuser internal surface. Downstream of the swirler, in a position at 80mm , the maximum horizontal speed is around 2 m/s, presenting a decline when the measurement is accomplished at 140 mm. When the flow enters in the diffuser, as shown in the measurements in diffuser cross sections in the Fig. 4, the maximum velocity component of the secondary flow is of the order of 1m/s at a distance of 30mm of the diffuser entrance, decreasing for about 0.7 m/s at a distance of 50 mm of its entrance. Fig. 5 and Fig. 6 show the results of the numerical simulation in the respective cross sections already shown for the experimental results, in other words, between the swirler and the diffuser and in the cross sections of the own diffuser.

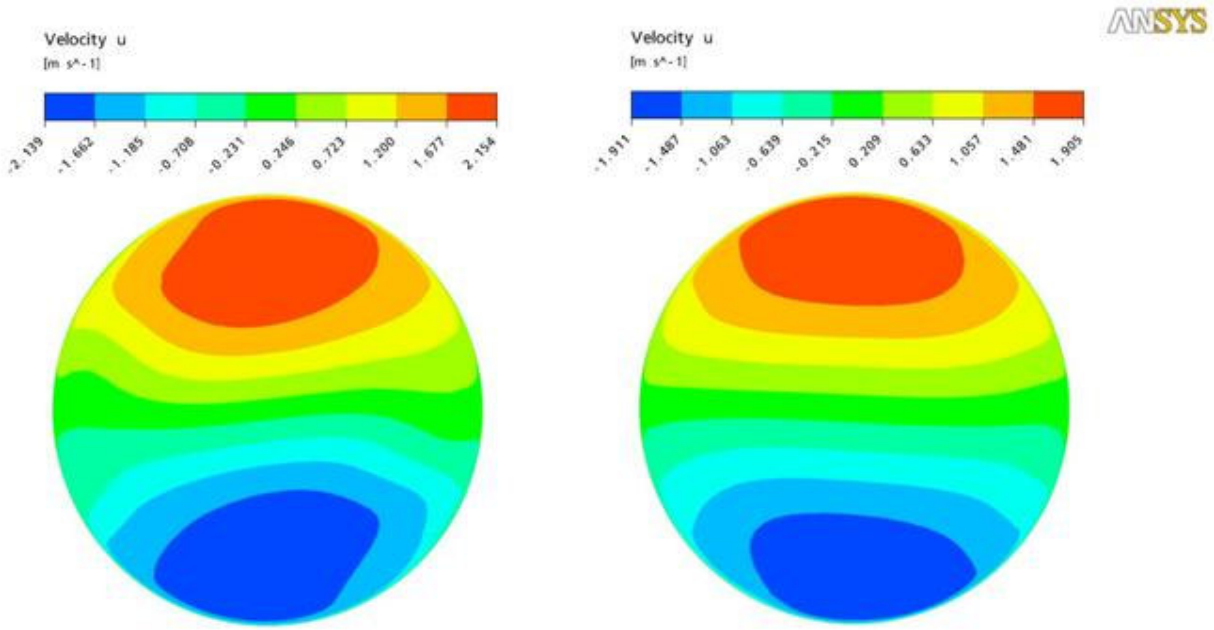

Figure 5: Horizontal velocity components for the de 20º diffuser, on the cross sections at 80 mm and 140 mm from the swirler.

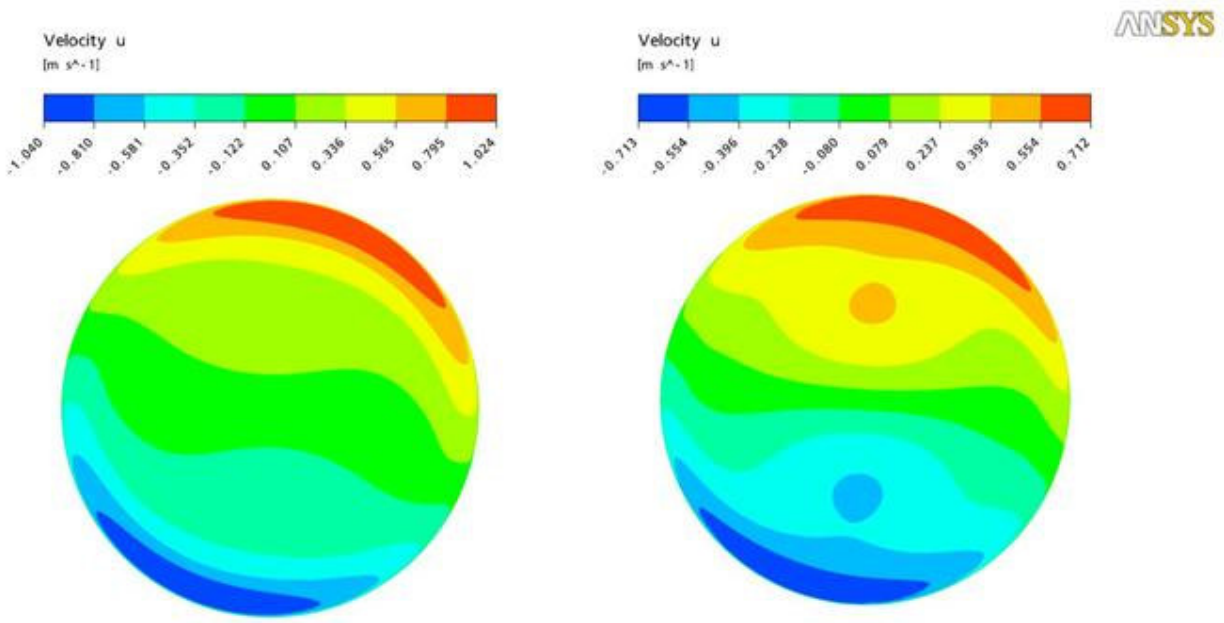

Figure 6: Horizontal velocity components inside the 20º diffuser, at cross sections at 80 mm and 140 mm from its entrance.

The simulated results, downstream of the swirler, on the cross sections at 80 mm and 140 mm, also present a swirling flow, with maximum horizontal speed of the order of 2.15 m/s and 1.9 m/s, respectively. Inside the diffuser, in the cross sections at 30 mm and 50 mm of its entrance, the horizontal maximum speed is of the order of 1.0 m/s and 0.7 m/s. The experimental and numerical results present very close values.

The Fig. 7 presents the longitudinal flow inside the diffuser of total angle equal to 20º. The experimental and numerical results show a diffuser operating with a large central recirculation zone. The numerical results present values of axial speed in this recirculation region with larger intensity than those obtained by the experiments. The more intense axial speeds occur in the entrance of the diffuser, in the regions close to the wall. The maximum values of these measured axial speeds are of the order of 1.4 m/s, while those obtained by simulation show values of the order of 2.4 m/s. In the recirculation region the experimental data present maximum axial speeds of the order of -0.2 m/s, while in the simulation they are around -0.6 m/s.

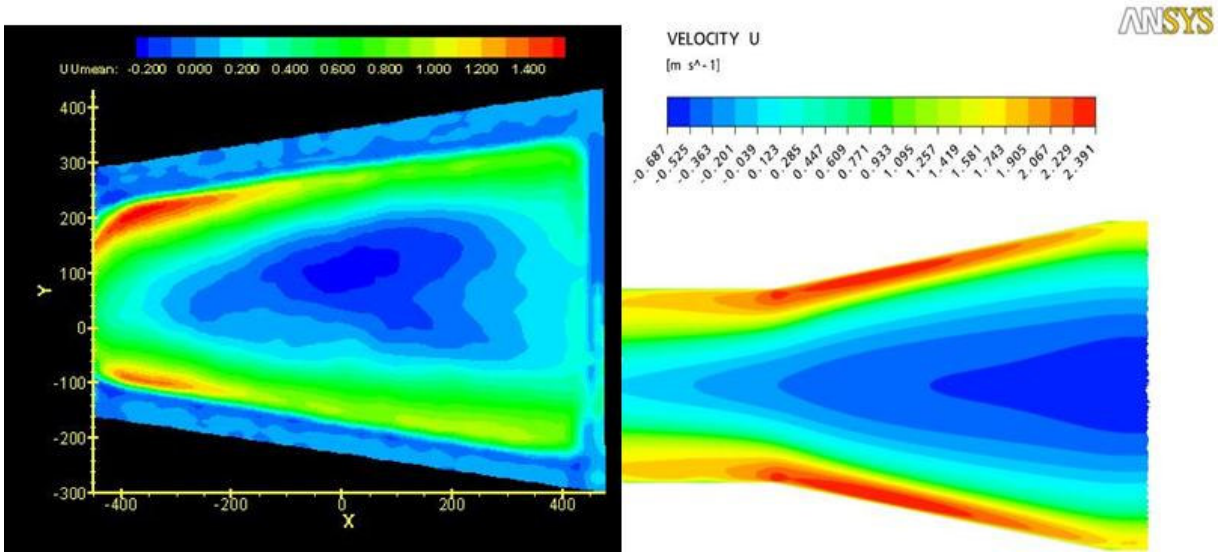

Figure 7: Longidinal flow inside the 20º diffuser. Axial velocities in m/s.

Fig. 8 and Fig. 9 show the experimental secondary flow in the diffuser of $10^{o.}$ In Fig. 8 the results refer to the positions of 90mm and 120mm downstream of the swirl. The swirl was installed, in this case, at 150 mm of the diffuser entrance.

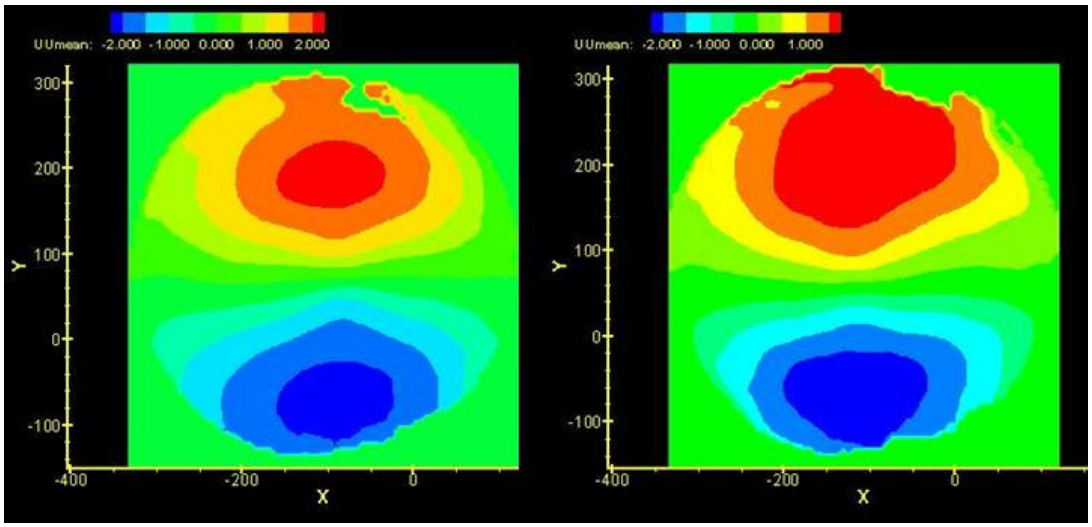

Figure 8: Horizontal velocity components for the de 10º diffuser.
Cross sections at 90 mm and 120 mm from the swirler exit .

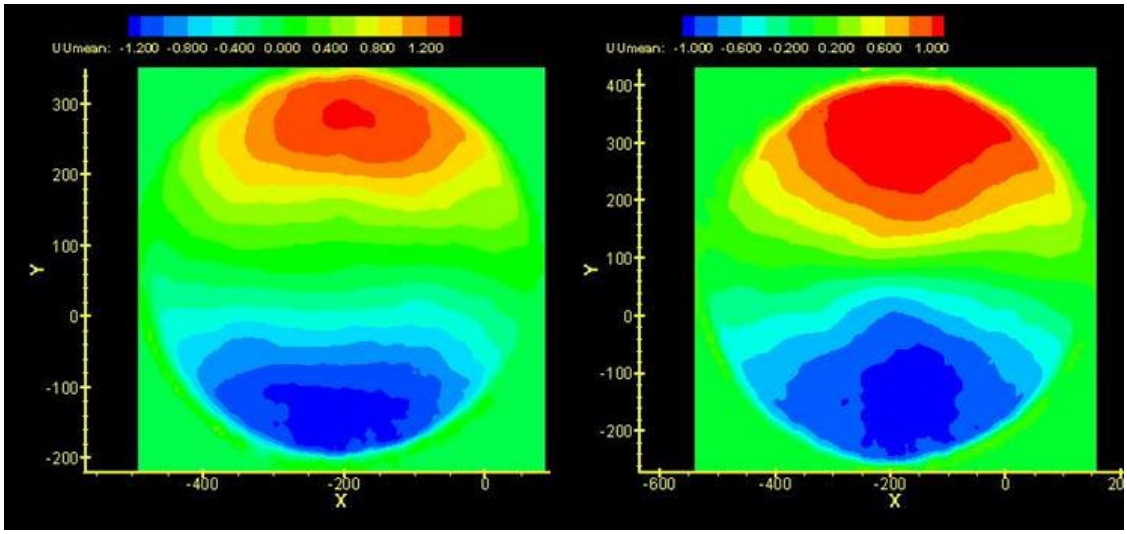

Figure 9: Horizontal velocity components inside the 10º diffuser. Cross sections at 55mm and 90mm of its entrance.

Fig. 10 and Fig. 11 show the respective simulated results in the cross sections between the swirl and the diffuser of total angle equal to 10º , and also in the own diffuser.

The secondary flow at 55 mm 90 mm of the swirler shows values of maximum horizontal speed very similar, while in the position to 90 mm of the swirler exit, the measured results are larger than the simulated data. The measurements in the diffuser, on the other hand, present higher values than those found in the numerical simulation for this tested diffuser geometry.

The Fig. 12 presents the experimental and numerical longitudinal velocities results, for the diffuser of total angle equals 10º. The experimental results are presented in two images, since the PIV acquisition system only cover an image surface of 60 mm x 60 mm and the total length of this diffuser is equal to 110 mm. The superposition of these two PIV images is equal to 5mm. Likely to the data found for the diffuser of total angle of 20^{o}, there is a large recirculation region dominating the diffuser flow. The experimental data show axial recirculation speeds of the order of -0.2 m/s in this region, while the results of the numerical simulation present maximum values of the order of -0.5 m/s. The

maximum axial positive speeds happen again in close regions of the diffuser wall, with experimental values of the order of 1.4 m/s and simulated data of the order of 2.15 m/s.

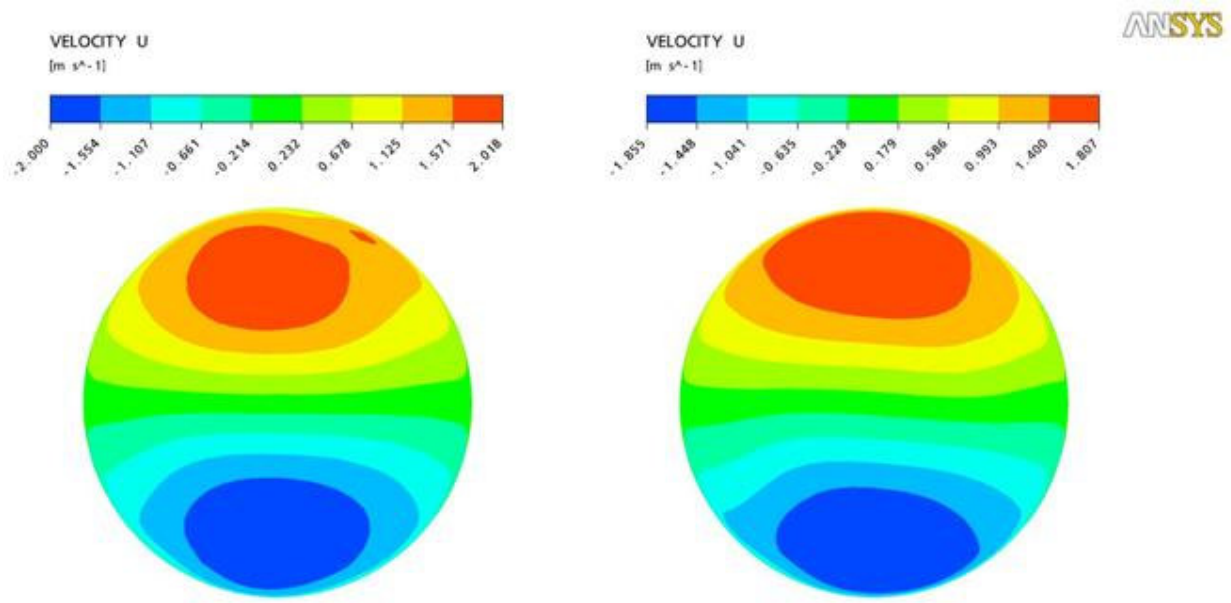

Figure 10: Simulated horizontal velocity components for the de 10º diffuser.
Cross sections at 90 mm and 120 mm from the swirler exit.

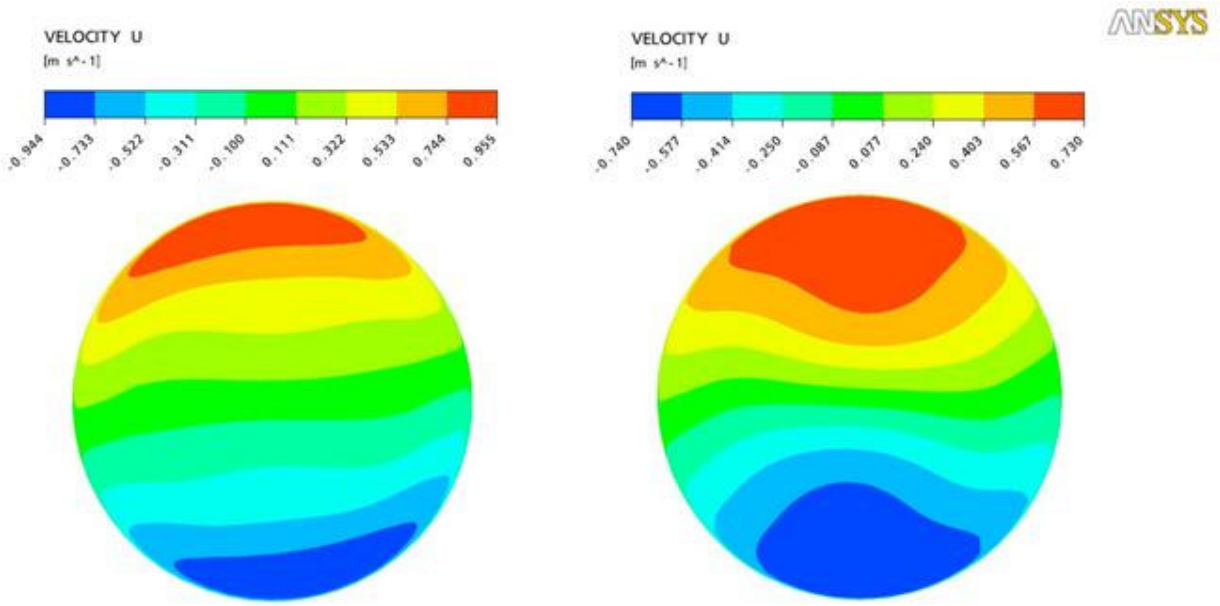

Figure 11: Simulated horizontal velocity components inside the 10º diffuser.
Cross sections at 55 mm and 90 mm of its entrance

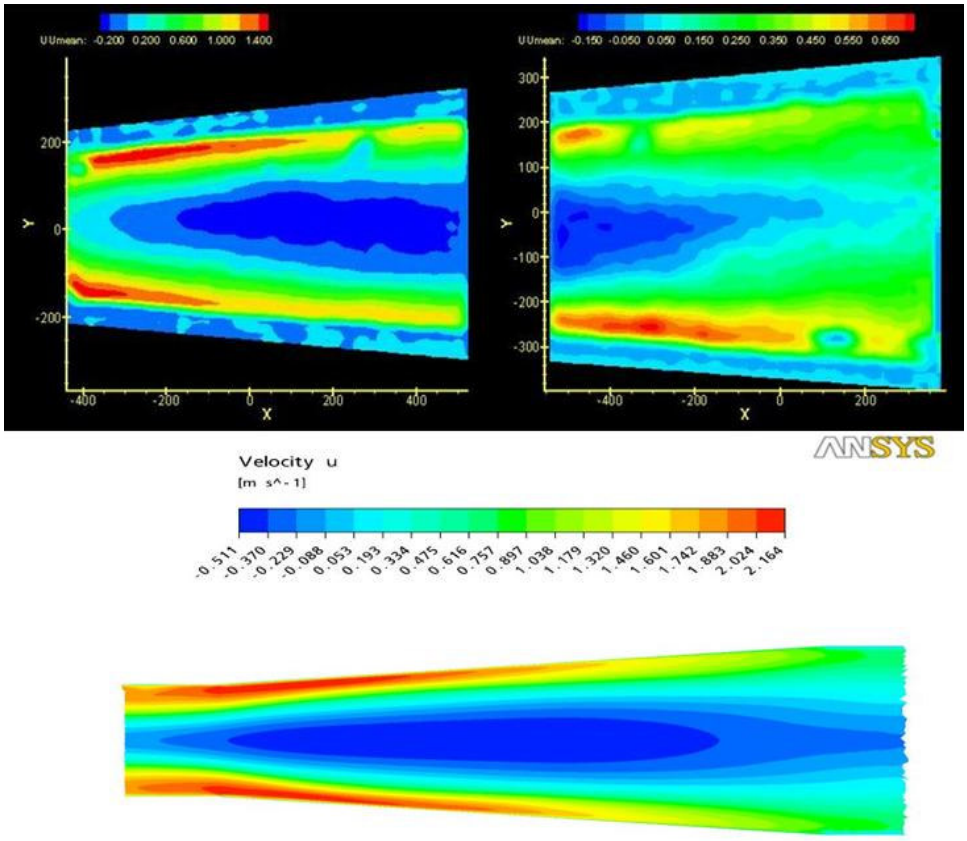

Figure 12: Longitudinal flow inside the diffuser of total angle equal to 10^0. Axial velocity im m/s.

5. CONCLUSIONS

The swirling flow in two different diffuser geometries were studied in the present work using Particle Image Velocimetry and Numerical Simulation with CFX. PIV has shown to be a good tool to study this very complex turbulent tridimensional flow. Numerical simulation, on the other hand, is able to show many aspects of this complex flow, that cannot be captured by experimental means. When comparisons between the experimental and simulated data are done, reasonable results are obtained. In this very complex swirling flow, superimposed to the rotating flow, it is also a Precessing Vortex Core – PVC, operating as a source of instabilities in the whole flow.

The objective of finding quantitative results was reached. In the future, it is intended to insert the transient term in the numerical analysis with the intention of detection with better precision the effects of that complex flow. Like this, the continuity of this work has a great challenge, to determine the effective robustness of the chosen numerical method in analyzing drainage with intense swirl variety, high pressure gradients and PVC.

6. ACKNOWLEDMENTS

This work received the financial support of the ELETRONORTE - R&D program.

7. REFERENCES

Armfis S. W., Cho N. and Fletcher A. J., 1990, “Prediction of Turbulence Quantities for Swirling flow in Conical Diffusers”, American Institute of Aeronautics and Astronautics, Vol. 23, No 3, pp. 453-460.

Avelan F., Mauri S. and Kueny J. L., 2000, “Numerical Prediction of the Flow in a Turbine Draft Tube Influence of the Boundary Conditions”, ASME 2000 Fluids Engineering Division Summer Meeting, Boston, Massachusetts, USA, 7 p.

Azad R. S. and Kassab, S.Z., 1989, "Turbulent flow in a conical diffuser: Overview and implications", Americal Institute of Phisics, A 1 (3), pp. 564 – 573

Balanço Energético Nacional, 2005, Ministério de Minas e Energia.

Berstron J. and Gebart R., 1999, "Estimation of Numerical Accuracy for the Flow Field in a Draft Tube", International Journal of Numerical Methods for Heat & Fluid Flow, Vol. 6, No. 4 pp. 472-486

Clausen, P. D., Kish, S. G. and Wood D. H., 1993, "Measurement of a Swirling Turbulent Boundary Layer Developing in a Conical Diffuser", Experimental Thermal and Fluid Science, Vol. 6, pp. 39-48.

Coelho, J. G., 2006, Dissertação de Mestrado, "Estudo Numérico de Tubos de Sucção de Turbinas Hidráulicas Tipo Bulbo", Universidade de Brasília, 110 p.

Coelho, J. G., Brasil, A. C. P. J., Simulação Numérica da Influência do Swirl em Difusores, 11th Brazilian Congress of Thermal Sciences and Engineering, ENCIT 2006, ABCM, Brasil.

Coelho, J. G., Noleto, L. G., e Brasil, A. C. P. J., Escoamentos Turbulentos em Difusores Cônicos – simulações Transientes, 5ª Escola de Primavera de Transição e Turbulência, EPTT 2006, ABCM, Brasil.

Dixon S. L., 1998, "Fluid Mechanics and Thermodynamics of Turbomachinery", Butterworth-Heinemann, England.

Grotjans H., 2001, "Simulation of Draft Tube Flow with CFX", Second ERCOFTAC Worshop on Draft Tube Flow, Vattenfall Utvercling AB, Älvkarleby, Sweden.

Henry P., 1992, "Turbomachines Hydrauliques", Presses Polytechniques et Universitaires Romandes, França, 407p.

Iaccarino G., 2000, "Prediction of the Turbulent Flow in a Diffuser with Commercial CFD Codes", Annual Research Briefs 2000, pp. 271-279.

Japikse D,2000, "Correlation of Annular Diffuser Performance with Geometry, Swirl, and Blockage", 11Th Thermal ans Fluid Analysis Worshop, Cleveland, Ohio.

Labrecque Y., Sabourin M. and Deschênes C., 1996, "Numerical Simulation of a Complete Turbine and Interaction Between Components", Modeliling, Testing & Monitoring for Hydro Poweplants, Lausanne, Switzerland.

Maliska, C. R., 2002, "Transferência de Calor e Mecânica dos Fluidos Computacionais", Livros Técnicos e Científicos Editora S.A., Rio de Janeiro, 424 p.

Menter F. R, 1994, "Two-equation eddy-viscosity turbulence models for engineering applications", AIAA Journal Vol. 32, pp 1598-1605.

Menter F. R., Kuntz, M., e Langtry, R., 2003, "Ten years of industrial experience with the SST turbulence model", Turbulence, heat and Mass transfer 4,8 p.

Puente L. R., "Reggio M. and Guibault F. 2001, Automatic Shape Optimization of a Hydraulic Turbine Draft Tube", Departament of Mechanical Engineering, 6 p.

Tamm A., Gugau M and Stoffel B., 2002, "Experimental and 3D Numerical Analysis of the Flow Field in Turbomachines Part I", International Congress on Quality Assessment of Numerical Simulations in Engineering, University of Conception, Chile.

Wilcox, D. C., 1993, "Turbulence Modelling for CFD", DWC Industries Inc., La Canada, 460p.

White F. M., 1994, "Fluid Mechanics", McGraw-Hill, Inc., London, 736p.

Zulcy S, abd Bran R., 1987, "Máquinas de Fluxo: Turbinas, Bombas, Ventiladores", Ao Livro Tecnico, Rio de Janeiro, 262p.

8. RESPONSIBILITY NOTICE

The authors are the only responsible for the printed material included in this paper.